Accuracy of finite differences in smooth media

Luděk Klimeš
Department of Geophysics, Charles University, Ke Karlovu 3, 121 16 Praha 2, Czech Republic, Fax: +42-2-299272, E-mail: psencik@earn.cvut.cz

Summary

Accuracy of finite–difference schemes of the 2^{nd} and 4^{th} order in 2-D and 3-D regular rectangular grids is studied. The method of designing the schemes and estimating their accuracy is proposed. Considered are the point schemes, expressed in terms of the values of the material parameters and of the wavefield at gridpoints. Only the common schemes applicable in smooth parts of seismic models, outside structural interfaces are taken into account. Finite differences at structural interfaces are studied in another paper.

The inaccuracy of finite–difference schemes is governed, above all, by the error in the propagation velocity, caused by the discretization. This error is estimated for several finite–difference schemes. It is explicitly dependent on the direction of propagation and on the wave polarization. The maximum propagation–velocity error over all directions of propagation enables to appreciate the accuracy of individual schemes in order to find the best one. The proposed approach is general, and applicable to other finite–difference schemes, for example, of the 6^{th} and higher orders.

Keywords

Seismic waves, finite differences of the 2^{nd} and 4^{th} order, 2-D and 3-D seismic modelling, elasticity.

1 Introduction

Accuracy of finite–difference schemes of the 2^{nd} and 4^{th} order in 2-D and 3-D regular rectangular grids is studied in this paper. Only the point schemes, expressed in terms of the values of the material parameters and of the wavefield at gridpoints, are considered.

The error analysis shows that, in smooth parts of the model, the most severe errors are due to the finite–difference approximation of the second space derivatives of the wavefield. Such errors cannot be reduced by the usage of some averaged "effective" material parameters. In this way, the application of purely point schemes inside geological blocks is justified.

Similarly, from the point of view of accuracy, the author sees no reason to consider staggered grids. The staggered grids suffer from less accurate approximation of the homogeneous (i.e. non–mixed) second partial wavefield derivatives. The inaccuracy is more pronounced for the finite–differences of a higher order, and also in 3-D.

In Sections 2 and 3, the method of designing the point finite–difference schemes applicable in smooth parts of seismic models, outside structural interfaces is presented. The method is suitable both in isotropic and anisotropic seismic models. The schemes have the general form of a linear operators acting on the wavefield gridpoint values. These finite–difference schemes may be generalized for the application in the vicinity of structural interfaces. The application at structural interfaces is presented in another paper in order to keep this paper concise and readable.

In Sections 4 and 5, the tools for estimating the accuracy of finite–difference schemes are presented. The inaccuracy of finite–difference schemes is governed especially by the error in the propagation velocity, caused by the discretization. The presented methods for estimating the accuracy of finite–difference schemes are applicable both in isotropic and anisotropic seismic models.

In Section 6, given are the accuracy and some other properties of several particular finite–difference approximations of individual partial wavefield derivatives ("partial schemes"). This analysis follows the method of Sections 2 and 3. The wavefield differencing is, of course, independent of anisotropy.

In Section 7, the relative propagation–velocity error due to the inaccurate second partial wavefield derivatives in isotropic models is estimated. This error is estimated for several finite–difference schemes of the 2^{nd} and 4^{th} order in 2-D and 3-D regular rectangular grids. It is explicitly dependent on the direction of propagation and on the wave polarization. The maximum propagation–velocity error over all directions of propagation enables to appreciate the accuracy of individual schemes in order to find the best one. Section 7 follows from Sections 5 and 6.

In Section 8, the relative propagation–velocity error due to the inaccurate first partial wavefield derivatives is estimated.

In Section 9, the relative propagation–velocity error due to the inaccurate first partial derivative of the material parameters is estimated.

The proposed approach is general, and applicable to other finite–difference schemes, for example, of the 6^{th} and higher orders.

2 Wavefield on a rectangular grid

2.1 Gridpoint values

At a time level, the wavefield is represented by gridpoint values $u_i(\mathbf{x})$, where the positional vector $\mathbf{x}$ takes the values (positions) of all gridpoints. In the computer memory, the gridpoints are, as a rule, indexed. Then the positional vector $\mathbf{x}$ is represented by the corresponding integer index, and $u_i(\mathbf{x})$ by an array.

Let us denote by $\mathbf{h}_i$ the vectorial grid intervals. If the grid is regular and rectangular in the Cartesian coordinates, and the grid interval in all directions is of the same length h, we may choose

$$\mathbf{h}_1 = (h,0,0)^{\mathrm{T}} \ , \quad \mathbf{h}_2 = (0,h,0)^{\mathrm{T}} \ , \quad \mathbf{h}_3 = (0,0,h)^{\mathrm{T}} \quad . \tag{1}$$

The gridpoints $\mathbf{y}$, from the vicinity of fixed gridpoint $\mathbf{x}$ situated inside the grid, may then be expressed in the form of

$$\mathbf{y} = \mathbf{x} + n_1\mathbf{h}_1 + n_2\mathbf{h}_2 + n_3\mathbf{h}_3 = \mathbf{x} + n_i\mathbf{h}_i \quad , \tag{2}$$

where n_1, n_2, and n_3 are small signed integers. For instance, $n_i = -1, 0, 1$ for 3-D finite differences of the second order, and $n_I = -1, 0, 1$, $n_3 = 0$ for 2-D finite differences of the second order. If the gridpoints are indexed, grid intervals $\mathbf{h}_1$, $\mathbf{h}_2$, $\mathbf{h}_3$ are represented by the corresponding shifts of the index. For example, if the grid values in the grid of dimensions $5 \times 4 \times 3$ are stored in the Fortran manner, $\mathbf{h}_1 = 1$, $\mathbf{h}_2 = 5$, and $\mathbf{h}_3 = 20$ in the computer representation.

2.2 Taylor expansion

For fixed gridpoint $\mathbf{x}$ situated inside the grid, we denote

$$u_{i(n_1,n_2,n_3)} = u_i(\mathbf{x} + n_1\mathbf{h}_1 + n_2\mathbf{h}_2 + n_3\mathbf{h}_3) \quad . \tag{3}$$

These grid values are the arguments of a linear finite–difference operator. Within the smooth geological block, the grid values may be approximated by the Taylor expansion from gridpoint $\mathbf{x}$.

Let us denote by

$$\begin{aligned}
&U_i = u_i(\mathbf{x}) \ , \quad U_{ij} = u_{i,j}(\mathbf{x}) = \frac{\partial u_i}{\partial x_j}(\mathbf{x}) \ , \quad U_{ijk} = u_{i,jk}(\mathbf{x}) = \frac{\partial^2 u_i}{\partial x_j \partial x_k}(\mathbf{x}) \ , \\
&U_{ijkl} = u_{i,jkl}(\mathbf{x}) = \frac{\partial^3 u_i}{\partial x_j \partial x_k \partial x_l}(\mathbf{x}) \ , \\
&U_{ijklm} = u_{i,jklm}(\mathbf{x}) = \frac{\partial^4 u_i}{\partial x_j \partial x_k \partial x_l \partial x_m}(\mathbf{x}) \ , \quad \ldots \quad .
\end{aligned} \tag{4}$$

the value and partial derivatives of the wavefield at $\mathbf{x}$. Then the gridpoint values (3) may be approximated by

$$u_{i(n_1,n_2,n_3)} = U_i + hU_{ij}n_j + \frac{h^2}{2}U_{ijk}n_jn_k + \frac{h^3}{6}U_{ijkl}n_jn_kn_l + \frac{h^4}{24}U_{ijklm}n_jn_kn_ln_m + \ldots \ . \tag{5}$$

We arrange, for fixed $\mathbf{x}$, the grid values (3) into vector $\mathbf{u}$, and the partial derivatives (4) into vector $\mathbf{U}$. Equal derivatives (e.g. U_{112} and U_{121}) are summed to form a single element of $\mathbf{U}$ (e.g. $U_{1[12]} = U_{112} + U_{121}$, where index $[i,j]$ corresponds to all permutations of i and j). Then the Taylor expansion (5) may be expressed as the linear transformation

$$\mathbf{u} = \mathbf{T}\mathbf{U} \quad , \tag{6}$$

where the elements of the Taylor–expansion matrix $\mathbf{T}$, projecting U_i, U_{ij}, $U_{i[jk]}$, $U_{i[jkl]}$, $U_{i[jklm]}$, ... onto $u_{n(n_1,n_2,n_3)}$, are

$$\begin{aligned}
&T_{n(n_1,n_2,n_3):i} = \delta_{ni} \ , \\
&T_{n(n_1,n_2,n_3):ij} = \delta_{ni} h n_j \ , \\
&T_{n(n_1,n_2,n_3):i[jk]} = \delta_{ni} \frac{h^2}{2} n_j n_k \ , \\
&T_{n(n_1,n_2,n_3):i[jkl]} = \delta_{ni} \frac{h^3}{6} n_j n_k n_l \ , \\
&T_{n(n_1,n_2,n_3):i[jklm]} = \delta_{ni} \frac{h^4}{24} n_j n_k n_l n_m \ , \quad \ldots \quad .
\end{aligned} \tag{7}$$

2.3 Second time derivatives of the wavefield

Let us consider general linear stress–strain relations

$$\sigma_{ij} = c_{ijkl} u_{k,l} \quad , \tag{8}$$

where c_{ijkl} are the elastic parameters. In an isotropic medium,

$$c_{ijkl} = \delta_{ij}\delta_{kl}\lambda + \delta_{ik}\delta_{jl}\mu + \delta_{il}\delta_{jk}\mu \quad , \tag{9}$$

where

$$\lambda = \varrho({v_{\rm P}}^2 - 2{v_{\rm S}}^2) \ , \quad \mu = \varrho {v_{\rm S}}^2 \quad . \tag{10}$$

The second partial time derivative of the wavefield is then

$$u_{i,tt} = \varrho^{-1} \frac{\partial \sigma_{ij}}{\partial x_j} = \varrho^{-1}(c_{ijkl} u_{k,lj} + c_{ijkl,j} u_{k,l}) \quad , \tag{11}$$

and specifically at $\mathbf{x}$

$$u_{i,tt}(\mathbf{x}) = \varrho^{-1}(C_{ijkl} U_{klj} + C_{ijklj} U_{kl}) \quad , \tag{12}$$

where

$$C_{ijkl} = c_{ijkl}(\mathbf{x}) \ , \quad C_{ijklm} = \frac{\partial c_{ijkl}}{\partial x_m}(\mathbf{x}) \tag{13}$$

are the values and partial derivatives of the elastic parameters at central point $\mathbf{x}$. In an isotropic medium,

$$C_{ijkl} U_{klj} = (\lambda + \mu)\, U_{kki} + \mu U_{ikk} \quad , \tag{14}$$

$$C_{ijklj} = \delta_{kl} \frac{\partial \lambda}{\partial x_i}(\mathbf{x}) + \delta_{il} \frac{\partial \mu}{\partial x_k}(\mathbf{x}) + \delta_{ik} \frac{\partial \mu}{\partial x_l}(\mathbf{x}) \quad , \tag{15}$$

and

$$C_{ijklj} U_{kl} = \frac{\partial \lambda}{\partial x_i}(\mathbf{x})\ U_{kk} + \frac{\partial \mu}{\partial x_k}(\mathbf{x})\ [U_{ik} + U_{ki}] \quad . \tag{16}$$

Partial derivatives C_{ijklm} of the elastic parameters at $\mathbf{x}$ may be estimated using symmetrical differences

$$C_{ijklm} = \frac{1}{2h}[c_{ijkl}(\mathbf{x} + \mathbf{h}_m) - c_{ijkl}(\mathbf{x} - \mathbf{h}_m)] \tag{17}$$

of the second order if all points $\mathbf{x} - \mathbf{h}_m$, $\mathbf{x}$, $\mathbf{x} + \mathbf{h}_m$ are situated in the same geological block. In other words, if the points are not separated by a structural interface. At structural interfaces, partial derivatives C_{ijklm} should preferably be calculated by the model–specification software instead of differencing.

Equation (12) is the linear dependence

$$\mathbf{t} = \mathbf{S}\mathbf{U} \tag{18}$$

of the vector

$$\mathbf{t} = (u_{1,tt}, u_{2,tt}, u_{3,tt})^{\rm T} \tag{19}$$

on the vector $\mathbf{U}$ of the partial derivatives. The only non–zero components of the matrix $\mathbf{S}$ are

$$S_{n\ ij} = \varrho^{-1} C_{ijnkk} \ , \quad S_{n\ ijk} = \varrho^{-1}(C_{ijkn} + C_{ikjn})/2 \quad , \tag{20}$$

projecting U_{ij} and $U_{i[jk]}$ onto $u_{n,tt}$, respectively.

3 Finite–difference schemes inside geological blocks

To determine the finite–difference scheme, we select N wavefield values at the gridpoints within the vicinity of each central point $\mathbf{x}$. These N values determine vector $\mathbf{u}$ of wavefield grid values. Equation (6) then represents N linear equations for the partial wavefield derivatives ordered in vector $\mathbf{U}$. We thus have to select N non–zero partial derivatives and put all other components of $\mathbf{U}$ equal zero. The partial wavefield derivatives up to the second order must not be annulled. The set of N non–zero components of $\mathbf{U}$ has to be selected in such a way that the resulting system (6) of N linear equations for N non–zero components of $\mathbf{U}$ is regular. Thus, in our approach, the finite–difference scheme will be fully determined by selecting the set of N gridpoint wavefield values (arguments of the scheme) and the set of N non–zero partial wavefield derivatives.

If choosing a reasonable subset $\mathbf{u}$ of grid values (3) and the corresponding reasonable subset $\mathbf{U}$ of partial derivatives (4), the Taylor–expansion matrix $\mathbf{T}$ may be inverted and equation (6) can be solved,

$$\mathbf{U} = \mathbf{T}^{-1}\mathbf{u} \quad . \tag{21}$$

From (7) it is obvious that inverse Taylor–expansion matrix $\mathbf{T}^{-1}$ is dependent only on the grid structure and on the selected size and structure of the vectors $\mathbf{u}$ and $\mathbf{U}$, i.e. on the choice of the finite–difference scheme. Moreover, for a regular grid, inverse Taylor–expansion matrix $\mathbf{T}^{-1}$ is the same for all "inner" gridpoints $\mathbf{x}$. The finite–difference schemes of "inner" gridpoints do not cross the grid boundaries or structural interfaces.

The finite–difference scheme inside a smooth geological block may now be expressed in the general matrix form of

$$\mathbf{t} = \mathbf{S}\mathbf{T}^{-1}\mathbf{u} \quad . \tag{22}$$

4 Accuracy of finite–difference schemes — basic concepts

4.1 Errors

Error $\delta(Q)$ of quantity Q is understood hereinafter as the deviation of approximately calculated value Q from value $\bar{Q}$ corresponding to the exact solution of the relevant equations,

$$\delta(Q) = Q - \bar{Q} \quad . \tag{23}$$

4.2 Asymptotic approximation of wavefield derivatives

First we introduce the parameters describing grid spacing with respect to the wavelength,

$$\epsilon_0 = -\mathrm{i}\frac{2\pi H}{T} \ , \quad \epsilon = \mathrm{i}\frac{2\pi h}{\Lambda} \quad , \tag{24}$$

where H is the time step, h is the grid step in space, T is the period, and Λ is the wavelength of a monochromatic wave. We also denote

$$\epsilon_i = \epsilon\vartheta_i \quad , \tag{25}$$

where ϑ_i are the components of the unit vector normal to the wavefront. The partial wavefield derivatives may then be roughly approximated by

$$u_i'' \simeq u_i \left(-\mathrm{i}\frac{2\pi}{T}\right)^2 = u_i \left(\frac{\epsilon_0}{H}\right)^2 = u_i \left(\frac{v\epsilon}{h}\right)^2 \quad , \tag{26}$$

and

$$U_{ijk...n} \simeq U_i \frac{\epsilon_j}{h} \frac{\epsilon_k}{h} ... \frac{\epsilon_n}{h} \quad . \tag{27}$$

We have denoted by $u_i'' = \partial^2 u_i / \partial t^2$ the second partial wavefield derivative with respect to time.

4.3 Relative propagation–velocity error

The error of the calculated wavefield is caused by the inaccuracy of the evaluation of the second derivative u_i'' of the wavefield with respect to time by means of the finite-differences in space, and by the inaccuracy of the finite–difference scheme of the second order along the time axis.

The main component of error $\delta(u_i'')$ in the second derivative u_i'' is the component along the polarization vector

$$e_i = U_i / \sqrt{U_m U_m} \quad . \tag{28}$$

This error, $e_i \delta(u_i'')$, influences considerably the calculated wavefield. Its real part causes the error in the propagation velocity along the ray and, consequently, in travel time, whereas its imaginary part causes the errors in the amplitude of the calculated waves. Let us emphasize that the imaginary part of the main error in u_i'' causes the same corresponding relative deviation from the exact solution, as the real part of the same magnitude does.

The additional components of error $\delta(u_i'')$ in the second derivative u_i'' are perpendicular to the polarization vector e_i. The additional components of error $\delta(u_i'')$ in the second derivative u_i'' locally disturb the polarization of the wavefield, but have no considerable influence on the propagation velocity nor the magnitude of the wavefield amplitudes, compared with the influence of the main component of the error. In opposite to the main component, the additional components of the error do not accumulate during the wave propagation. Thus, the additional components of error $\delta(u_i'')$ in the second derivative u_i'' may usually be neglected.

The error of $\delta(u_i'')$ in u_i'' causes the relative complex–valued error of

$$\Delta = \frac{1}{2} \frac{u_i \delta(u_i'')}{u_m u_m''} \tag{29}$$

in the propagation velocity of the wavefront along the ray. Because of (26), the above error may be approximated by

$$\Delta \simeq \frac{1}{2} \frac{H^2}{\epsilon_0^2} \frac{u_i \delta(u_i'')}{u_m u_m} = \frac{1}{2} \frac{h^2}{v^2 \epsilon^2} \frac{u_i \delta(u_i'')}{u_m u_m} \quad . \tag{30}$$

4.4 Distortion of monochromatic waves

The resulting relative error Δ_u of the monochromatic wavefield u_i, $\delta(u_i) \simeq u_i \Delta_u$, accumulated during time t along the ray of the length s, is

$$\Delta_u \simeq -\mathrm{i}\frac{2\pi}{T}\int\limits_0^s \frac{\Delta}{v}\mathrm{d}s = -\mathrm{i}\frac{2\pi}{T}\int\limits_0^t \Delta \mathrm{d}t \quad . \tag{31}$$

This error accumulates with increasing time of propagation and there is a time level at which interference waves cannot be evaluated correctly. Thus, the relative propagation–velocity error should be chosen inverse proportional to the time interval of finite–difference calculation.

For example, if the average relative propagation velocity error is 10^{-3}, the relative error of the calculated wavefield at time $t = 10\,T$ is about 6%, at time $t = 40\,T$ about 25%. If the average relative propagation velocity error is 10^{-2}, the relative error of the calculated wavefield at time $t = 8\,T$ is about 50%.

4.5 Distortion of wave packets

The relative propagation–velocity error Δ increases with the K^{th} power of frequency $f = T^{-1}$, where K is the order of the finite difference scheme, $K = 2$ or $K = 4$. Then the wavefronts of the wave packet propagate along the ray with the relative velocity error of Δ approximately corresponding to the prevailing frequency, whereas the packet envelope propagates with the relative group–velocity error of

$$\Delta_{\mathrm{G}} = \Delta + f\frac{\mathrm{d}\Delta}{\mathrm{d}f} = (K+1)\Delta \quad . \tag{32}$$

Thus the erroneous time shift of the packet envelope, caused by the real part of the relative propagation–velocity error, is $(K+1)$-times greater than the time shift of the wavefronts. This causes the phase shift of the wave packet of

$$\delta(\phi) \simeq -K\frac{2\pi}{T}\int\limits_0^t \mathrm{Re}(\Delta)\mathrm{d}t \quad . \tag{33}$$

Similarly, the relative amplitude error of the packet envelope, caused by the imaginary part of the relative propagation–velocity error, is approximately $(K+1)$-times greater than the relative error of the amplitude of the monochromatic wave of the same prevailing frequency.

5 Sources of the relative propagation–velocity error

5.1 Error due to finite–differences of the second order with respect to time

First, we shall study the error of the finite–difference scheme

$$u_i(\mathbf{x}, t+H) = 2u_i(\mathbf{x}, t) - u_i(\mathbf{x}, t-H) + H^2 u_i''(\mathbf{x}, t) \tag{34}$$

along the time axis.

The error of this scheme is caused by neglecting the fourth derivative u_i'''' with respect to time on the right–hand side. The error in u_i'' due to neglecting term $2\frac{H^4}{24}u_i''''$ is

$$\delta(u_i'') \simeq -\frac{H^2}{12}u_i'''' \simeq -\frac{H^2}{12}u_i\left(\frac{\epsilon_0}{H}\right)^4 = -\frac{H^{-2}}{12}u_i\epsilon_0^4 \quad . \tag{35}$$

Substituting this estimate into (30) we arrive at the relative propagation–velocity error of

$$\Delta^{(0)} \simeq -\frac{1}{24}\epsilon_0^2 \tag{36}$$

corresponding to the second–order scheme (34). For example, if choosing 40 time steps per one period, $H = T/40$, the relative phase velocity error is 10^{-3}, whereas for 13 time steps per one period, $H = T/13$, the relative phase velocity error is 10^{-2}. The relative group velocity error is 3 times greater and, e.g., for $H = T/13$ the erroneous phase shift of wave packets at time $t = 13\,T$ is about $\pi/2$. However, this error may, to some extent, be eliminated by means of time and phase corrections applied to the Gabor transforms of synthetic seismograms.

5.2 Error due to finite–differences in space

The error of (12) is

$$\delta(u_i'') = \delta(\rho^{-1}C_{ijkl})U_{klj} + \rho^{-1}C_{ijkl}\delta(U_{klj}) + \rho^{-1}C_{ijklj}\delta(U_{kl}) + \delta(\rho^{-1}C_{ijklj})U_{kl} \ . \tag{37}$$

The values ρ^{-1} and C_{ijkl} of material parameters are assumed to be exact, $\delta(\rho^{-1}) = 0$ and $\delta(C_{ijkl}) = 0$, and the wavefield derivatives may be approximated by (27). Then

$$\delta(u_i'') = \rho^{-1}C_{ijkl}\delta(U_{klj}) + \rho^{-1}C_{ijklj}\delta(U_{kl}) + \rho^{-1}\delta(C_{ijklj})U_k\epsilon_l h^{-1} \quad . \tag{38}$$

Substituting this into (30), we arrive at

$$\Delta - \Delta^{(0)} \simeq \frac{1}{2}\frac{1}{\rho v^2\epsilon^2}\frac{U_i}{U_m U_m}\left[C_{ijkl}\delta(U_{klj})h^2 + C_{ijklj}\delta(U_{kl})h^2 + \delta(C_{ijklj})U_k\epsilon_l h\right] \ . \tag{39}$$

Assuming that the errors $\delta(U_{ij})$ and $\delta(U_{ijk})$ of the first and second wavefield derivatives may be expressed in terms of the corresponding relative errors Δ_j and Δ_{jk} of the finite–difference scheme,

$$\delta(U_{ij}) = U_{ij}\Delta_j \simeq U_i\epsilon_j h^{-1}\Delta_j \quad , \tag{40}$$

$$\delta(U_{ijk}) = U_{ijk}\Delta_{jk} \simeq U_i\epsilon_j\epsilon_k h^{-2}\Delta_{jk} \quad , \tag{41}$$

where no summation is taken over indices j and k, we arrive at

$$\Delta - \Delta^{(0)} \simeq \frac{1}{2}\frac{1}{\rho v^2 \epsilon^2}\frac{U_i}{U_m U_m} \times \left[\sum_{l=1}^{3}\sum_{j=1}^{3} C_{ijkl} U_k \epsilon_l \epsilon_j \Delta_{lj} + \sum_{l=1}^{3} C_{ijklj} U_k \epsilon_j h \Delta_l + \delta(C_{ijklj}) U_k \epsilon_l h\right] \quad . \quad (42)$$

The total relative propagation–velocity error may then be expressed in the form of

$$\Delta = \Delta^{(0)} + \Delta^{(1)} + \Delta^{(2)} + \Delta^{(3)} \quad , \quad (43)$$

with

$$\Delta^{(1)} \simeq \frac{1}{2}\frac{1}{\rho v^2 \epsilon^2} e_i e_k \sum_{l=1}^{3}\sum_{j=1}^{3} C_{ijkl} \epsilon_l \epsilon_j \Delta_{lj} \quad (44)$$

being the relative propagation–velocity error caused by the inaccurate second partial wavefield derivatives,

$$\Delta^{(2)} \simeq \frac{1}{2}\frac{h}{\rho v^2 \epsilon^2} e_i e_k \sum_{l=1}^{3} C_{ijklj} \epsilon_l \Delta_l \quad (45)$$

being the relative propagation–velocity error caused by the inaccurate first partial wavefield derivatives, and

$$\Delta^{(3)} \simeq \frac{1}{2}\frac{h}{\rho v^2 \epsilon^2} e_i e_k \delta(C_{ijklj}) \epsilon_l \quad (46)$$

being the relative propagation–velocity error caused by the inaccurate first partial derivatives of the elastic parameters.

These contributions $\Delta^{(1)}$, $\Delta^{(2)}$, and $\Delta^{(3)}$ to the whole relative propagation–velocity error Δ will be estimated in the next sections.

6 Partial finite–difference schemes

As mentioned above, the only partial wavefield derivatives at $\mathbf{x}$, appearing in equation (12) and thus influencing the time development of the wavefield, are the first and second derivatives U_{ij} and $U_{i[jk]}$.

Thus, we shall first study the relative errors Δ_j of U_{ij}, and Δ_{jk} of $U_{i[jk]}$, in the approximation (21). Since the approximations of individual partial derivatives in (21) are, to some extent, independent for most of symmetric finite–difference schemes, we may decompose the finite–difference schemes into several partial schemes for individual partial derivatives, and to estimate the relative error of each partial derivative independently. These results will then be used to estimate the relative propagation velocity errors of the waves of particular polarizations (P, S_1, and S_2) in several finite–difference schemes.

6.1 Partial scheme, 1-D, 3-point, 2 nd order

Wavefield grid values (arguments):

$$u_{i(n_1,0,0)},\ n_1 = -1, 0, +1 \quad . \tag{47}$$

Determined Taylor–expansion coefficients:

$$U_i, U_{i1}, U_{i[11]} \quad . \tag{48}$$

Most important neglected Taylor–expansion coefficients:

$$U_{i[111]}, U_{i[1111]} \quad . \tag{49}$$

Finite–difference equation for the first partial derivative inside a geological block (*2 floating–point operations* per hU_{i1}, or *1 floating–point operation* per $2hU_{i1}$):

$$hU_{i1} = \frac{1}{2}[u_{i(+1,0,0)} - u_{i(-1,0,0)}] \quad . \tag{50}$$

Finite–difference equation for the second partial derivative inside a geological block (*3 floating–point operations* per $h^2U_{i[11]}$):

$$h^2U_{i[11]} = u_{i(+1,0,0)} + u_{i(-1,0,0)} - 2u_{i(0,0,0)} \quad . \tag{51}$$

Relative error in $hU_{i1} \simeq U_i\epsilon_1$ due to neglecting $h^3U_{i[111]} \simeq U_i\epsilon_1^3$ inside geological blocks:

$$\Delta_1 = \frac{1}{\epsilon_1}\frac{1}{2}\,[1+1]\,\frac{\epsilon_1^3}{6} = \frac{1}{6}\epsilon_1^2 \quad . \tag{52}$$

Relative error in $h^2U_{i[11]} \simeq U_i\epsilon_1^2$ due to neglecting $h^4U_{i[1111]} \simeq U_i\epsilon_1^4$ inside geological blocks:

$$\Delta_{11} = \frac{1}{\epsilon_1^2}\,[1+1]\,\frac{\epsilon_1^4}{24} = \frac{1}{12}\epsilon_1^2 \quad . \tag{53}$$

Analogously in the directions of the 2nd and 3rd coordinate axes,

$$\Delta_j = \frac{1}{6}\epsilon_j^2 \quad , \tag{54}$$

$$\Delta_{j=k} = \frac{1}{12}\epsilon_j^2 \quad . \tag{55}$$

6.2 Partial scheme, 1-D, 5-point, 4^{th} order

Wavefield grid values (arguments):

$$u_{i(n_1,0,0)},\ n_1 = -2,-1,0,+1,+2 \quad . \tag{56}$$

Determined Taylor–expansion coefficients:

$$U_i, U_{i1}, U_{i[11]}, U_{i[111]}, U_{i[1111]} \quad . \tag{57}$$

Most important neglected Taylor–expansion coefficients:

$$U_{i[11111]}, U_{i[111111]} \quad . \tag{58}$$

Finite–difference equation for the first partial derivative inside a geological block (*5 floating–point operations* per hU_{i1}, or *4 floating–point operation* per $12hU_{i1}$):

$$hU_{i1} = \frac{1}{12}[8(u_{i(+1,0,0)} - u_{i(-1,0,0)}) - (u_{i(+2,0,0)} - u_{i(-2,0,0)})] \quad . \tag{59}$$

Finite–difference equation for the second partial derivative inside a geological block (*7 floating–point operations* per $h^2U_{i[11]}$):

$$h^2U_{i[11]} = \frac{1}{12}[16(u_{i(+1,0,0)} + u_{i(-1,0,0)}) - (u_{i(+2,0,0)} + u_{i(-2,0,0)}) - 30u_{i(0,0,0)}] \quad . \tag{60}$$

Relative error in $hU_{i1} \simeq U_i\epsilon_1$ due to neglecting $h^5U_{i[11111]} \simeq U_i\epsilon_1^5$ inside geological blocks:

$$\Delta_1 = \frac{1}{\epsilon_1}\frac{1}{12}\left[8(1+1) - (32+32)\right]\frac{\epsilon_1^5}{120} = -\frac{1}{30}\epsilon_1^4 \quad . \tag{61}$$

Relative error in $h^2U_{i[11]} \simeq U_i\epsilon_1^2$ due to neglecting $h^6U_{i[111111]} \simeq U_i\epsilon_1^6$ inside geological blocks:

$$\Delta_{11} = \frac{1}{\epsilon_1^2}\frac{1}{12}\left[16(1+1) - (64+64)\right]\frac{\epsilon_1^6}{720} = -\frac{1}{90}\epsilon_1^4 \quad . \tag{62}$$

Analogously in the directions of the 2^{nd} and 3^{rd} coordinate axes,

$$\Delta_j = -\frac{1}{30}\epsilon_j^4 \quad , \tag{63}$$

$$\Delta_{j=k} = -\frac{1}{90}\epsilon_j^4 \quad . \tag{64}$$

6.3 Partial scheme, 2-D, 4-point, 2nd order

This scheme for the mixed second derivatives is equivalent to the double application of the partial 1-D 3-point scheme (50) for the first derivatives.

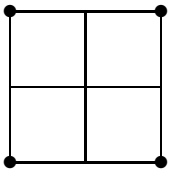

Wavefield grid values (arguments):

$$u_{i(\pm 1,\pm 1,0)} \quad . \tag{65}$$

Determined Taylor–expansion coefficients in addition to 1-D partial schemes:

$$U_{i[12]}, U_{i[112]}, U_{i[122]}, U_{i[1122]} \quad . \tag{66}$$

Most important neglected Taylor–expansion coefficients in addition to 1-D partial schemes:

$$U_{i[1112]}, U_{i[1222]}, U_{i[11112]}, U_{i[11122]}, U_{i[11222]}, U_{i[12222]} \quad . \tag{67}$$

Finite–difference equation for the second partial derivative inside a geological block:

$$2h^2 U_{i12} = h^2 U_{i[12]} = \frac{1}{2}[u_{i(+1,+1,0)} - u_{i(-1,+1,0)} - u_{i(+1,-1,0)} + u_{i(-1,-1,0)}] \quad . \tag{68}$$

This could take *4 floating–point operations*. However, if having stored the first derivatives resulting from (50), the evaluation of (68) by means of the second application of (50) takes only additional *2 floating–point operations*.
Relative error in $h^2 U_{i[12]} \simeq 2U_i\epsilon_1\epsilon_2$ due to neglecting $h^4 U_{i[1112]} \simeq 4U_i\epsilon_1^3\epsilon_2$ and $h^4 U_{i[1222]} \simeq 4U_i\epsilon_1\epsilon_2^3$ inside geological blocks:

$$\Delta_{12} = \frac{1}{2\epsilon_1\epsilon_2}\frac{1}{2}[1+1+1+1]\left(\frac{4\epsilon_1^3\epsilon_2}{24} + \frac{4\epsilon_1\epsilon_2^3}{24}\right) = \frac{1}{6}(\epsilon_1^2 + \epsilon_2^2) \quad . \tag{69}$$

Analogously in the x_1x_3 and x_2x_3 planes,

$$\Delta_{j\neq k} = \frac{1}{6}(\epsilon_j^2 + \epsilon_k^2) \quad , \tag{70}$$

that, of course, corresponds to errors (54) of the double application of (50) in directions j and k.

6.4 Partial scheme, 2-D, 8-point, 4^{th} order (3^{rd} order)

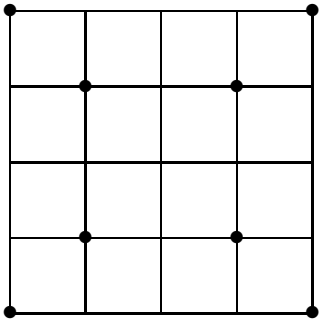

Wavefield grid values (arguments):

$$u_{i(\pm1,\pm1,0)},\ u_{i(\pm2,\pm2,0)} \quad . \tag{71}$$

Determined Taylor–expansion coefficients in addition to 1-D 5-point partial schemes:

$$U_{i[12]}, U_{i[112]}, U_{i[122]}, U_{i[1122]}, U_{i[1112]} + U_{i[1222]},$$

$$U_{i[11112]} + U_{i[11222]}, U_{i[11122]} + U_{i[12222]},$$

$$U_{i[111111]} + U_{i[111122]} + U_{i[112222]} + U_{i[222222]} \quad . \tag{72}$$

Most important neglected Taylor–expansion coefficients in addition to 1-D 5-point partial schemes:

$$U_{i[1112]} - U_{i[1222]}, U_{i[11112]} - U_{i[11222]}, U_{i[11122]} - U_{i[12222]},$$

$$U_{i[111111]} - U_{i[111122]}, U_{i[111111]} - U_{i[112222]}, U_{i[111111]} - U_{i[222222]},$$

$$U_{i[111112]}, U_{i[111222]}, U_{i[122222]} \quad . \tag{73}$$

Finite–difference equation for the second partial derivative inside a geological block (*9 floating–point operations* per $h^2 U_{i[12]}$):

$$\begin{aligned} 2h^2 U_{i12} = h^2 U_{i[12]} = \frac{1}{24}[16(&u_{i(+1,+1,0)} - u_{i(-1,+1,0)} - u_{i(+1,-1,0)} + u_{i(-1,-1,0)}) \\ &-(u_{i(+2,+2,0)} - u_{i(-2,+2,0)} - u_{i(+2,-2,0)} + u_{i(-2,-2,0)})] \ . \end{aligned} \tag{74}$$

Relative error in $h^2 U_{i[12]} \simeq 2U_i\epsilon_1\epsilon_2$ due to neglecting $h^6 U_{i[111112]} \simeq 6U_i\epsilon_1^5\epsilon_2$, $h^6 U_{i[111222]} \simeq 20U_i\epsilon_1^3\epsilon_2^3$, and $h^6 U_{i[122222]} \simeq 6U_i\epsilon_1\epsilon_2^5$ inside geological blocks:

$$\begin{aligned} \Delta_{12} &= \frac{1}{2\epsilon_1\epsilon_2}\frac{1}{24}[16(1+1+1+1) - (64+64+64+64)]\left(\frac{6\epsilon_1^5\epsilon_2^1}{720} + \frac{20\epsilon_1^3\epsilon_2^3}{720} + \frac{6\epsilon_1\epsilon_2^5}{720}\right) \\ &= -\frac{1}{180}\left(6\epsilon_1^4 + 20\epsilon_1^2\epsilon_2^2 + 6\epsilon_2^4\right) \ . \end{aligned} \tag{75}$$

Analogously in the x_1x_3 and x_2x_3 planes,

$$\Delta_{j\neq k} = -\frac{1}{180}(6\epsilon_j^4 + 20\epsilon_j^2\epsilon_k^2 + 6\epsilon_k^4) \quad . \tag{76}$$

6.5 Partial scheme, 2-D, 12-point, 4^{th} order

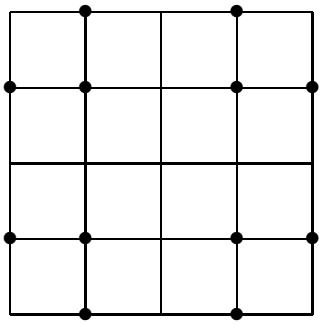

Wavefield grid values (arguments):

$$u_{i(\pm1,\pm1,0)},\ u_{i(\pm2,\pm1,0)},\ u_{i(\pm1,\pm2,0)} \quad . \tag{77}$$

Determined Taylor–expansion coefficients in addition to 1-D 5-point partial schemes:

$$U_{i[12]}, U_{i[112]}, U_{i[122]}, U_{i[1112]}, U_{i[1122]}, U_{i[1222]},$$

$$U_{i[11112]}, U_{i[11122]}, U_{i[11222]}, U_{i[12222]}, U_{i[111122]}, U_{i[112222]} \quad . \tag{78}$$

Most important neglected Taylor–expansion coefficients in addition to 1-D 5-point partial schemes:

$$U_{i[111112]}, U_{i[111222]}, U_{i[122222]},$$

$$U_{i[1111112]}, U_{i[1111122]}, U_{i[1111222]}, U_{i[1112222]}, U_{i[1122222]}, U_{i[1222222]} \quad . \tag{79}$$

Finite–difference equation for the second partial derivative inside a geological block (*13 floating–point operations* per $h^2 U_{i[12]}$):

$$\begin{aligned} 2h^2 U_{i12} = h^2 U_{i[12]} = \frac{1}{12}[10(&u_{i(+1,+1,0)} - u_{i(-1,+1,0)} - u_{i(+1,-1,0)} + u_{i(-1,-1,0)}) \\ &-(u_{i(+2,+1,0)} - u_{i(-2,+1,0)} - u_{i(+2,-1,0)} + u_{i(-2,-1,0)}) \\ &-(u_{i(+1,+2,0)} - u_{i(-1,+2,0)} - u_{i(+1,-2,0)} + u_{i(-1,-2,0)})] \ . \end{aligned} \tag{80}$$

Relative error in $h^2 U_{i[12]} \simeq 2U_i\epsilon_1\epsilon_2$ due to neglecting $h^6 U_{i[111112]} \simeq 6U_i\epsilon_1^5\epsilon_2$, $h^6 U_{i[111222]} \simeq 20U_i\epsilon_1^3\epsilon_2^3$, and $h^6 U_{i[122222]} \simeq 6U_i\epsilon_1\epsilon_2^5$ inside geological blocks:

$$\begin{aligned} \Delta_{12} = \frac{1}{2\epsilon_1\epsilon_2}\frac{1}{12}\Bigg[&(10*4-4*32-4*2)*\frac{6\epsilon_1^5\epsilon_2}{720} + (10*4-4*8-4*8)*\frac{20\epsilon_1^3\epsilon_2^3}{720} \\ &+(10*4-4*2-4*32)*\frac{6\epsilon_1\epsilon_2^5}{720}\Bigg] = -\frac{1}{180}(6\epsilon_1^4 + 5\epsilon_1^2\epsilon_2^2 + 6\epsilon_2^4) \ . \end{aligned} \tag{81}$$

Analogously in the x_1x_3 and x_2x_3 planes,

$$\Delta_{j\neq k} = -\frac{1}{180}(6\epsilon_j^4 + 5\epsilon_j^2\epsilon_k^2 + 6\epsilon_k^4) \quad . \tag{82}$$

6.6 Partial scheme, 2-D, 16-point, 4^{th} order

This scheme for the mixed second derivatives is equivalent to the double application of the partial 1-D 5-point scheme (59) for the first derivatives.

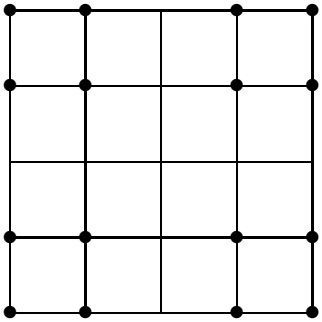

Wavefield grid values (arguments):

$$u_{i(\pm1,\pm1,0)},\ u_{i(\pm2,\pm1,0)},\ u_{i(\pm1,\pm2,0)},\ u_{i(\pm2,\pm2,0)} \quad . \tag{83}$$

Determined Taylor–expansion coefficients in addition to 1-D 5-point partial schemes:

$$U_{i[12]}, U_{i[112]}, U_{i[122]}, U_{i[1112]}, U_{i[1122]}, U_{i[1222]}, U_{i[11112]}, U_{i[11122]}, U_{i[11222]}, U_{i[12222]},$$
$$U_{i[111122]}, U_{i[111222]}, U_{i[112222]}, U_{i[1111222]}, U_{i[1112222]}, U_{i[11112222]} \quad . \tag{84}$$

Most important neglected Taylor–expansion coefficients in addition to 1-D 5-point partial schemes:

$$U_{i[111112]}, U_{i[122222]}, U_{i[1111112]}, U_{i[1111122]}, U_{i[1122222]}, U_{i[1222222]} \quad . \tag{85}$$

Finite–difference equation for the second partial derivative inside a geological block:

$$\begin{aligned} 2h^2U_{i12} = h^2U_{i[12]} = \frac{1}{9}[8(&u_{i(+1,+1,0)} - u_{i(-1,+1,0)} - u_{i(+1,-1,0)} + u_{i(-1,-1,0)}) \\ &-(u_{i(+2,+1,0)} - u_{i(-2,+1,0)} - u_{i(+2,-1,0)} + u_{i(-2,-1,0)}) \\ &-(u_{i(+1,+2,0)} - u_{i(-1,+2,0)} - u_{i(+1,-2,0)} + u_{i(-1,-2,0)})] \\ &+\tfrac{1}{8}(u_{i(+2,+2,0)} - u_{i(-2,+2,0)} - u_{i(+2,-2,0)} + u_{i(-2,-2,0)})] \ . \end{aligned} \tag{86}$$

This could take *18 floating–point operations*. However, if having stored the first derivatives resulting from (59), the evaluation of (86) by means of the second application of (59) takes only additional *5 floating–point operations*.

Relative error in $h^2U_{i[12]} \simeq 2U_i\epsilon_1\epsilon_2$ due to neglecting $h^6U_{i[111112]} \simeq 6U_i\epsilon_1^5\epsilon_2$, and $h^6U_{i[122222]} \simeq 6U_i\epsilon_1\epsilon_2^5$ inside geological blocks:

$$\begin{aligned} \Delta_{12} = \frac{1}{2\epsilon_1\epsilon_2}\frac{1}{9}\Bigg[&(8*4-4*32-4*2+\frac{1}{8}*4*64)*\frac{6\epsilon_1^5\epsilon_2}{720} \\ &+(8*4-4*2-4*32+\frac{1}{8}*4*64)*\frac{6\epsilon_1\epsilon_2^5}{720}\Bigg] = -\frac{1}{180}(6\epsilon_1^4+6\epsilon_2^4) \ . \end{aligned} \tag{87}$$

Analogously in the x_1x_3 and x_2x_3 planes,

$$\Delta_{j\neq k} = -\frac{1}{180}(6\epsilon_j^4 + 6\epsilon_k^4) \quad . \tag{88}$$

that, of course, corresponds to errors (63) of the double application of (50) in directions j and k.

7 Error due to the inaccurate second partial wavefield derivatives

In this section, we shall study the relative propagation–velocity errors of the most important 2-D and 3-D finite–difference schemes on regular rectangular grids in smooth isotropic media. Let us emphasize that the usage of staggered grids seems to be unreasonable from our point of view.

The relative error of the propagation velocity v of the wave of a particular polarization (P, S_1, or S_2), caused by the inaccurate second partial wavefield derivatives, is given by (44) and is real–valued.

In an isotropic medium, see (9), equation (44) reads

$$\begin{aligned}\Delta^{(1)} &\simeq \frac{1}{2}\frac{\sum_{j,k}[(\lambda+\mu)e_j e_k + \mu\delta_{jk}]\epsilon_j\epsilon_k\Delta_{jk}}{\rho v^2\epsilon^2} \\ &= \frac{1}{2}\frac{\sum_{j,k}[({v_{\mathrm{P}}}^2 - {v_{\mathrm{S}}}^2)e_j e_k + {v_{\mathrm{S}}}^2\delta_{jk}]\epsilon_j\epsilon_k\Delta_{jk}}{v^2\epsilon^2} \\ &= \frac{1}{2v^2}\left\{\sum_j[({v_{\mathrm{P}}}^2 - {v_{\mathrm{S}}}^2)e_j^2 + {v_{\mathrm{S}}}^2]\epsilon_j^2\Delta_{jj} + 2\sum_{j<k}({v_{\mathrm{P}}}^2 - {v_{\mathrm{S}}}^2)e_j e_k\epsilon_j\epsilon_k\Delta_{jk}\right\}\epsilon^{-2}\,. \quad (89)\end{aligned}$$

Now the relative errors corresponding to the particular finite–difference schemes have to be substituted for Δ_{jk}.

7.1 2-D, 9-point, 2nd order

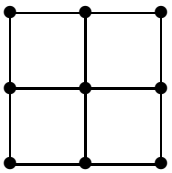

This scheme is composed of 1-D 3-point and 2-D 4-point partial schemes, and costs *10 to 14 floating–point operations* × *2 components*, depending on the quantities stored in the memory. Equation (89) reads

$$\Delta^{(1)} \simeq \frac{1}{24v^2}\left\{\sum_j[({v_{\mathrm{P}}}^2 - {v_{\mathrm{S}}}^2)e_j^2 + {v_{\mathrm{S}}}^2]\epsilon_j^4 + 4\sum_{j<k}({v_{\mathrm{P}}}^2 - {v_{\mathrm{S}}}^2)e_j e_k(\epsilon_j^3\epsilon_k + \epsilon_j\epsilon_k^3)\right\}\epsilon^{-2}\,. \quad (90)$$

Maximum relative P-wave propagation velocity error for ${v_{\mathrm{P}}}^2 \le 3{v_{\mathrm{S}}}^2$ arises along the gridline,

$$\Delta^{(1)}_{\max} = \frac{1}{24}\epsilon^2 \quad . \quad (91)$$

Maximum relative P-wave propagation velocity error for ${v_{\mathrm{P}}}^2 \ge 3{v_{\mathrm{S}}}^2$ is greater and arises along the diagonal,

$$\Delta^{(1)}_{\max} = \frac{1}{24}\left(\frac{5}{4} - \frac{3}{4}\frac{{v_{\mathrm{S}}}^2}{{v_{\mathrm{P}}}^2}\right)\epsilon^2 \quad . \quad (92)$$

Maximum relative S-wave propagation velocity error for ${v_{\mathrm{P}}}^2 \le 3{v_{\mathrm{S}}}^2$ arises along the gridline,

$$\Delta^{(1)}_{\max} = \frac{1}{24}\epsilon^2 \quad . \quad (93)$$

Maximum relative S-wave propagation velocity error for ${v_\mathrm{P}}^2 \geq 3{v_\mathrm{S}}^2$ is greater and arises along the diagonal,

$$\Delta^{(1)}_{\max} = -\frac{1}{24}\left(\frac{3}{4}\frac{{v_\mathrm{P}}^2}{{v_\mathrm{S}}^2} - \frac{5}{4}\right)\epsilon^2 \quad . \tag{94}$$

7.2 2-D, 17-point, 4^{th} order

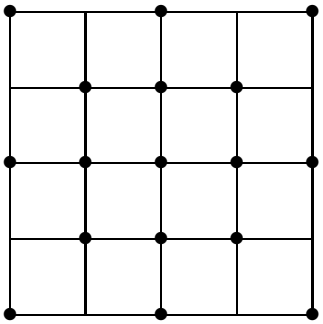

This scheme is composed of 1-D 5-point and 2-D 8-point partial schemes, and costs *31 to 33 floating–point operations* $\times$ *2 components*, depending on the quantities stored in the memory. Equation (89) reads

$$\Delta^{(1)} \simeq -\frac{1}{180v^2}\left\{\sum_j [({v_\mathrm{P}}^2 - {v_\mathrm{S}}^2)e_j^2 + {v_\mathrm{S}}^2]\epsilon_j^6 + \sum_{j<k}({v_\mathrm{P}}^2 - {v_\mathrm{S}}^2)e_j e_k(6\epsilon_j^5\epsilon_k + 20\epsilon_j^3\epsilon_k^3 + 6\epsilon_j\epsilon_k^5)\right\}\epsilon^{-2} \ . \tag{95}$$

Maximum relative P-wave propagation velocity error for ${v_\mathrm{P}}^2 \leq \frac{5}{3}{v_\mathrm{S}}^2$ arises along the gridline,

$$\Delta^{(1)}_{\max} = -\frac{1}{180}\epsilon^4 \quad . \tag{96}$$

Maximum relative P-wave propagation velocity error for ${v_\mathrm{P}}^2 \geq \frac{5}{3}{v_\mathrm{S}}^2$ is greater and arises along the diagonal,

$$\Delta^{(1)}_{\max} = -\frac{1}{180}\left(\frac{17}{8} - \frac{15}{8}\frac{{v_\mathrm{S}}^2}{{v_\mathrm{P}}^2}\right)\epsilon^4 \quad , \tag{97}$$

that is, e.g., for ${v_\mathrm{P}}^2 = 3{v_\mathrm{S}}^2$,

$$\Delta^{(1)}_{\max} = -\frac{1}{180}\frac{3}{2}\epsilon^4 \quad . \tag{98}$$

Maximum relative S-wave propagation velocity error for ${v_\mathrm{P}}^2 \leq \frac{5}{3}{v_\mathrm{S}}^2$ arises along the gridline,

$$\Delta^{(1)}_{\max} = -\frac{1}{180}\epsilon^4 \quad . \tag{99}$$

Maximum relative S-wave propagation velocity error for ${v_\mathrm{P}}^2 \geq \frac{5}{3}{v_\mathrm{S}}^2$ is greater and arises along the diagonal,

$$\Delta^{(1)}_{\max} = \frac{1}{180}\left(\frac{15}{8}\frac{{v_\mathrm{P}}^2}{{v_\mathrm{S}}^2} - \frac{17}{8}\right)\epsilon^4 \quad , \tag{100}$$

that is, e.g., for ${v_\mathrm{P}}^2 = 3{v_\mathrm{S}}^2$,

$$\Delta^{(1)}_{\max} = \frac{1}{180}\frac{7}{2}\epsilon^4 \quad . \tag{101}$$

7.3 2-D, 21-point, 4^{th} order

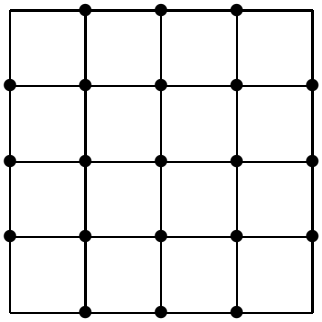

This scheme is composed of 1-D 5-point and 2-D 12-point partial schemes, and costs *35 to 37 floating–point operations* $\times$ *2 components*, depending on the quantities stored in the memory. Equation (89) reads

$$\Delta^{(1)} \simeq -\frac{1}{180v^2}\left\{\sum_j [({v_{\rm P}}^2 - {v_{\rm S}}^2)e_j^2 + {v_{\rm S}}^2]\epsilon_j^6 \right. \\ \left. + \sum_{j<k}({v_{\rm P}}^2 - {v_{\rm S}}^2)e_j e_k(6\epsilon_j^5\epsilon_k + 5\epsilon_j^3\epsilon_k^3 + 6\epsilon_j\epsilon_k^5)\right\}\epsilon^{-2} \ . \quad (102)$$

Maximum relative P-wave propagation velocity error for ${v_{\rm P}}^2 \leq 5{v_{\rm S}}^2$ arises along the gridline,

$$\Delta^{(1)}_{\max} = -\frac{1}{180}\epsilon^4 \quad . \quad (103)$$

Maximum relative P-wave propagation velocity error for ${v_{\rm P}}^2 \geq 5{v_{\rm S}}^2$ is greater and arises along the diagonal,

$$\Delta^{(1)}_{\max} = -\frac{1}{180}\left(\frac{19}{16} - \frac{15}{16}\frac{{v_{\rm S}}^2}{{v_{\rm P}}^2}\right)\epsilon^4 \quad . \quad (104)$$

Maximum relative S-wave propagation velocity error for ${v_{\rm P}}^2 \leq \frac{7}{3}{v_{\rm S}}^2$ arises along the gridline,

$$\Delta^{(1)}_{\max} = -\frac{1}{180}\epsilon^4 \quad . \quad (105)$$

Maximum relative S-wave propagation velocity error for ${v_{\rm P}}^2 \geq \frac{7}{3}{v_{\rm S}}^2$ is greater and arises along the diagonal,

$$\Delta^{(1)}_{\max} = \frac{1}{180}\left(\frac{15}{16}\frac{{v_{\rm P}}^2}{{v_{\rm S}}^2} - \frac{19}{16}\right)\epsilon^4 \quad , \quad (106)$$

that is, e.g., for ${v_{\rm P}}^2 = 3{v_{\rm S}}^2$,

$$\Delta^{(1)}_{\max} = \frac{1}{180}\frac{13}{8}\epsilon^4 \quad . \quad (107)$$

Thus this scheme is computationally slower but more accurate than the preceding 17-point scheme.

7.4 2-D, 25-point, 4^{th} order

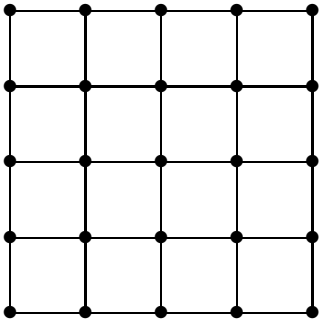

This scheme is composed of 1-D 5-point and 2-D 16-point partial schemes, and costs *27 to 42 floating–point operations* $\times$ *2 components*, depending on the quantities stored in the memory. Equation (89) reads

$$\Delta^{(1)} \simeq -\frac{1}{180v^2}\left\{\sum_j [({v_{\rm P}}^2 - {v_{\rm S}}^2)e_j^2 + {v_{\rm S}}^2]\epsilon_j^6 + \sum_{j<k}({v_{\rm P}}^2 - {v_{\rm S}}^2)e_j e_k(6\epsilon_j^5\epsilon_k + 6\epsilon_j\epsilon_k^5)\right\}\epsilon^{-2} \quad . \tag{108}$$

Maximum relative P-wave propagation velocity error arises along the gridline,

$$\Delta^{(1)}_{\rm max} = -\frac{1}{180}\epsilon^4 \quad . \tag{109}$$

Maximum relative S-wave propagation velocity error for ${v_{\rm P}}^2 \leq 3{v_{\rm S}}^2$ arises along the gridline,

$$\Delta^{(1)}_{\rm max} = -\frac{1}{180}\epsilon^4 \quad . \tag{110}$$

Maximum relative S-wave propagation velocity error for ${v_{\rm P}}^2 \geq 3{v_{\rm S}}^2$ is greater and arises along the diagonal,

$$\Delta^{(1)}_{\rm max} = \frac{1}{180}\left(\frac{5}{8}\frac{{v_{\rm P}}^2}{{v_{\rm S}}^2} - \frac{7}{8}\right)\epsilon^4 \quad . \tag{111}$$

Thus, in an isotropic medium, this scheme is both computationally faster and more accurate, for both P-waves and S-waves, than the preceding 17-point and 21-point schemes. The disadvantage of this scheme is that the the first wavefield derivatives are to be evaluated two grid intervals ahead and kept in the memory.

7.5 3-D, 19-point, 2^{nd} order

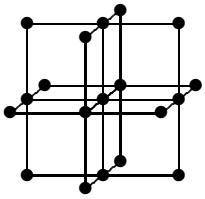

This scheme is composed of 1-D 3-point and 2-D 4-point partial schemes, and costs *18 to 27 floating–point operations* $\times$ *3 components*, depending on the quantities stored in the memory. Moreover, looking at (14), we see that not all 3 mixed second derivatives of all 3 wavefield components are needed. It is sufficient to calculate only

$$\frac{\partial}{\partial x^1}\left(u_{2,2}+u_{3,3}\right)\ ,\quad \frac{\partial}{\partial x^2}\left(u_{1,1}+u_{3,3}\right)\ ,\quad \frac{\partial}{\partial x^3}\left(u_{1,1}+u_{2,2}\right) \tag{112}$$

by means of the second application of (50). In this way, the costs may be decreased even to *14 floating–point operations* $\times$ *3 components*. Only the operations necessary to evaluate individual partial derivatives have been taken into account here.

The accuracy is the same as of the *2-D, 9-point,* 2^{nd} *order* scheme, see (90) to (94).

7.6 3-D, 37-point, 4^{th} order

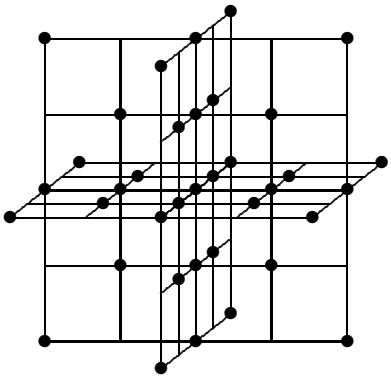

This scheme is composed of 1-D 5-point and 2-D 8-point partial schemes, and costs *60 to 63 floating–point operations* $\times$ *3 components*, depending on the quantities stored in the memory.

The accuracy is the same as of the *2-D, 17-point,* 4^{th} *order* scheme, see (95) to (101).

7.7 3-D, 49-point, 4^{th} order

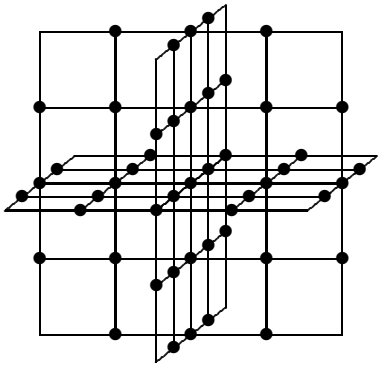

This scheme is composed of 1-D 5-point and 2-D 12-point partial schemes, and costs *72 to 75 floating–point operations* × *3 components*, depending on the quantities stored in the memory.

The accuracy is the same as of the *2-D, 21-point, 4*$^{\text{th}}$ *order* scheme, see (102) to (107).

7.8 3-D, 65-point, 4$^{\text{th}}$ order

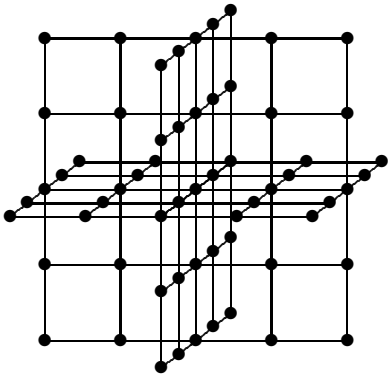

This scheme is composed of 1-D 5-point and 2-D 16-point partial schemes, and costs *48 to 90 floating–point operations* × *3 components*, depending on the quantities stored in the memory. Moreover, looking at (14), we see that not all 3 mixed second derivatives of all 3 wavefield components are needed. It is sufficient to calculate only

$$\frac{\partial}{\partial x^1}\left(u_{2,2}+u_{3,3}\right)\ ,\quad \frac{\partial}{\partial x^2}\left(u_{3,3}+u_{1,1}\right)\ ,\quad \frac{\partial}{\partial x^3}\left(u_{1,1}+u_{2,2}\right) \tag{113}$$

by means of the second application of (59). In this way, the costs may be decreased even to *38 floating–point operations* × *3 components* if $U_{22}+U_{33}$, $U_{33}+U_{11}$, and $U_{11}+U_{22}$ are stored in the memory. Only the operations necessary to evaluate individual partial derivatives have been taken into account here, unlike additions in (113).

The accuracy is the same as of the *2-D, 25-point, 4*$^{\text{th}}$ *order* scheme, see (108) to (111).

8 Error due to the inaccurate wavefield gradient

Substituting (54) into (45), we arrive at the estimation

$$\Delta^{(2)} \simeq \frac{1}{12}\frac{h}{\rho v^2\epsilon^2}e_i e_k \sum_{l=1}^{3} C_{ijklj}(\epsilon_l)^3 \tag{114}$$

of the relative propagation–velocity error due to the approximation of the wavefield gradient by the finite differences of the second order. Similarly, substituting (63) into (45), we arrive at the estimation

$$\Delta^{(2)} \simeq -\frac{1}{60}\frac{h}{\rho v^2\epsilon^2}e_i e_k \sum_{l=1}^{3} C_{ijklj}(\epsilon_l)^5 \tag{115}$$

of the relative propagation–velocity error due to the approximation of the wavefield gradient by the finite differences of the fourth order.

In an isotropic medium, the relative propagation–velocity error is

$$\Delta^{(2)} \simeq \frac{1}{12}\frac{h}{\rho v^2 \epsilon^2}\sum_{l=1}^{3}\frac{\partial(\rho v^2)}{\partial x_l}(\epsilon_l)^3 \quad , \tag{116}$$

for the finite differences of the 2^{nd} order, and

$$\Delta^{(2)} \simeq -\frac{1}{60}\frac{h}{\rho v^2 \epsilon^2}\sum_{l=1}^{3}\frac{\partial(\rho v^2)}{\partial x_l}(\epsilon_l)^5 \quad . \tag{117}$$

for the finite differences of the 4^{th} order.

If we denote, in an isotropic medium,

$$\frac{1}{L^{(1)}} = \max\left(\left|\frac{1}{\rho v^2}\frac{\partial(\rho v^2)}{\partial x_j}\right|,\ j=1,2,3\right) \quad , \tag{118}$$

the maximum absolute value of the imaginary relative propagation–velocity error due to the inaccurate wavefield gradient is

$$\Delta^{(2)}_{\max} \simeq \frac{|\epsilon|}{12}\frac{h}{L^{(1)}} \quad , \tag{119}$$

for the finite differences of the 2^{nd} order, and

$$\Delta^{(2)}_{\max} \simeq \frac{|\epsilon|^3}{60}\frac{h}{L^{(1)}} \quad . \tag{120}$$

for the finite differences of the 4^{th} order. This maximum error is reached if the wave propagates along the corresponding gridline.

9 Error due to the inaccurate gradient of material parameters

The error of approximation (17) is

$$\delta(C_{ijklm}) \simeq \frac{h^2}{6}\frac{\partial^3 c_{ijkl}}{(\partial x_m)^3}(\mathbf{x}) \quad . \tag{121}$$

Substituting (121) into (46) we arrive at

$$\Delta^{(3)} \simeq \frac{1}{12}\frac{h^3}{\rho v^2 \epsilon^2} e_i e_k \epsilon_l \sum_{j=1}^{3}\frac{\partial^3 c_{ijkl}}{(\partial x_j)^3}(\mathbf{x}) \quad . \tag{122}$$

In an isotropic medium, the relative propagation–velocity error is

$$\Delta^{(3)} \simeq \frac{1}{12}\frac{h^3}{\rho v^2 \epsilon^2}\sum_{j=1}^{3}\epsilon_j\frac{\partial^3(\rho v^2)}{(\partial x_j)^3} \quad . \tag{123}$$

If we denote, in an isotropic medium,

$$\frac{1}{L^{(3)}} = \max\left(\left|\frac{1}{\rho v^2}\frac{\partial^3(\rho v^2)}{(\partial x_j)^3}\right|,\ j=1,2,3\right) \quad , \tag{124}$$

the maximum absolute value of the imaginary relative propagation–velocity error due to the inaccurate gradient of the elastic parameters is

$$\Delta^{(3)}_{\max} \simeq \frac{1}{12|\epsilon|}\frac{h^3}{L^{(3)}} \quad . \tag{125}$$

This relative propagation–velocity error causes the error of the order of $\frac{1}{12}\frac{h^2}{L^{(2)}}$, with

$$\frac{1}{L^{(2)}} = \max\left(\left|\frac{1}{\rho v^2}\frac{\partial^2(\rho v^2)}{(\partial x_j)^2}\right|,\ j=1,2,3\right) \quad , \tag{126}$$

in the wavefield amplitudes, independently of the wavelength. Such an error should be negligible in all reasonably sampled models, independently of the order of finite–difference scheme used.

Warning

The author has not been able to find extremes of functions (90), (95), (102), and (108). In order to arrive at quantitative conclusions, the global extremes (91) to (94), (96) to (101), (103) to (107), and (109) to (111) have been found by an intuitive "trials and errors" approach and are not proved.